JACS
JOURNAL OF THE AMERICAN CHEMICAL SOCIETY
Article
pubs.acs.org/JACS

Bicarbonate and Alkyl Carbonate Radicals: Structural Integrity and Reactions with Lipid Components

Michael Bühl,* Peter DaBell, David W. Manley,† Rory P. McCaughan, and John C. Walton*

University of St. Andrews, EaStCHEM School of Chemistry, St. Andrews, Fife KY16 9ST, United Kingdom

Supporting Information

ABSTRACT: The elusive neutral bicarbonate radical and the carbonate radical anion form an acid/conjugate base pair. We now report experimental studies for a model of bicarbonate radical, namely, methyl carbonate (methoxycarbonyloxyl) radical, complemented by DFT computations at the CAM-B3LYP level applied to the bicarbonate radical itself. Methyl carbonate radicals were generated by UV irradiation of oxime carbonate precursors. Kinetic EPR was employed to measure rate constants and Arrhenius parameters for their dissociation to CO_2 and methoxyl radicals. With oleate and cholesterol lipid components, methyl carbonate radicals preferentially added to their double bonds; with linoleate and linolenate substrates, abstraction of the bis-allylic H atoms competed with addition. This contrasts with the behavior of ROS such as hydroxyl radicals that selectively abstract allylic and/or bis-allylic H atoms. The thermodynamic and activation parameters for bicarbonate radical dissociation, obtained from DFT computations, predicted it would indeed have substantial lifetime in gas and nonpolar solvents. The acidity of bicarbonate radicals was also examined by DFT methods. A noteworthy linear relationship was discovered between the known pK_a's of strong acids and the computed numbers of microsolvating water molecules needed to bring about their ionization. DFT computations with bicarbonate radicals, solvated with up to eight water molecules, predicted that only five water molecules were needed to bring about its complete ionization. On comparing with the correlation, this indicated a pK_a of about −2 units. This marks the bicarbonate radical as the strongest known carboxylic acid.

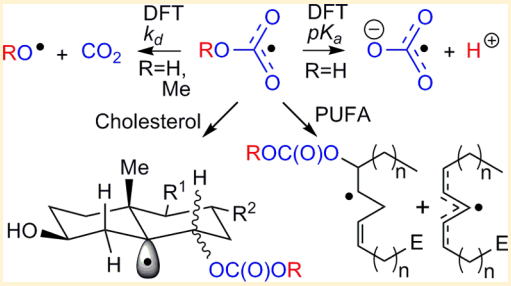

INTRODUCTION

Carbonic acid is a weak, diprotic acid formed upon dissolution of carbon dioxide in water. While its acid/base equilibria are well-understood, its radical chemistry is not. Deprotonations produce the bicarbonate anion HCO_3^- (pK_a = 6.38) and then carbonate dianion CO_3^{2-} (pK_a = 10.25) (Scheme 1).

Scheme 1. Formation of Carbonic Acid and Associated Anions and Radicals

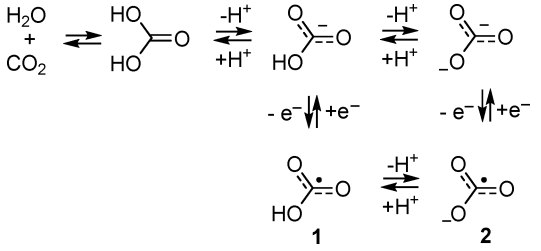

These species play important roles in geology, oceanology, atmospheric chemistry, and, of course, physiology. In blood serum and intracellular media, these equilibria constitute the bicarbonate buffer system. This is critical for maintaining the pH constant within the range 7.35−7.45, which is essential for optimum functioning of enzymes.[1] Approximately 70% of CO_2 is transported as bicarbonate in the human body (25.0 mM in serum and 14.4 mM in intracellular media).[2] When an electron is removed from bicarbonate or carbonate, respectively, neutral bicarbonate radicals **1** or carbonate radical anions **2** are created. There are several enzymatic (and possibly nonenzymatic) ways that these radicals can be produced in biological fluids. For example, CO_2 is one of peroxynitrite's primary biological targets, producing NO_2 and **2**.[3] Xanthine oxidase turnover of acetaldehyde and other substrates is also known to produce **2**.[4] Similarly, it is recognized[5] that the Cu,Zn-superoxide dismutase/H_2O_2 system also generates **2**.

As shown in Scheme 1, the carbonate radical anion **2** forms a conjugate base/acid pair with the neutral bicarbonate radical **1**. Apart from attempts to determine its pK_a, virtually nothing is known about the chemistry or biochemistry of the neutral bicarbonate radical itself. It was shown to be a strong acid,[6] and a computational study[7] suggested that its pK_a might be as low as −4 units. Because of this acidity, it is generally assumed that carbonate radical anions **2** are the dominant partner of the pair in biological fluids. Carbonate radical anion **2** is a reactive oxygen species (ROS) that contributes to oxidative stress.[8] It is an important oxidizing agent in aqueous solution,[9] and its main biotargets are polar species such as biothiols, nucleic acids, metalloproteins/proteins, and glutathione.[10]

Received: October 13, 2015
Published: December 1, 2015

DOI: 10.1021/jacs.5b10693
J. Am. Chem. Soc. 2015, 137, 16153−16162

Because $HOCO_2^•$ is neutral, whereas $^-OCO_2^•$ is negatively charged, and the two radicals have very different extents of electron delocalization, their preferred reaction channels and reactivity are expected to be markedly different. Thus, **2** is lipophobic, with the majority of its physiological reactions taking place in polar environments. Therefore, it should be a poor initiator of lipid peroxidation due to its low diffusibility in hydrophobic environments. The neutral protonated radical **1** could well be the dominant form in nonpolar hydrophobic lipid-rich situations. Initiation of peroxidation is the likely role of **1** in structures such as membranes, vesicles, low-density lipoprotein particles (LDL), or lipid microdomains. However, as of yet, there is no research reporting peroxidation of lipids by **1**. One reason for this is that the carbonate and bicarbonate precursors of **1** are soluble only in polar solvents so that even when **1** is formed it immediately deprotonates to **2**. No lipid-soluble precursor for **1** is currently known. To understand oxidative lipid and cell damage, with the resultant functional decline and associated degenerative conditions, a thorough study of the chemistry and biochemistry of both components of the carbonate/bicarbonate radical pair is much needed.

Radical **1** may be viewed as the first member of a homologous series with alkyl carbonate radicals:

$$HOC(O)O,\ MeOC(O)O,\ C_nH_{2n-1}OC(O)O$$

These neutral alkyl carbonate radicals are structurally similar to **1**, so they, and particularly the methyl carbonate radical (**7**), are suitable models for **1**. Several members of this series have been generated, and precursors soluble in organic solvents, that is, dialkyl peroxydicarbonates[11] and oxime carbonates,[12] are known. However, to our knowledge, the simplest member, methyl carbonate, has not yet been reported.

The objectives of this research were, first, to weigh up lipid-soluble precursors for radical **1** and, second, to investigate the structural integrity of **1** and of model $MeOC(O)O^•$ and related species, particularly with respect to the ease with which they decarboxylate:

$$R^1OC(O)O^• \rightarrow R^1O^• + CO_2$$

An examination of specific reactions of these species with lipid components was also a priority. In each case, both experimental and quantum-mechanical (QM) computational methods were employed. By these means, insight into the reactivity of model $MeOC(O)O^•$ and of radicals **1** and **2**, as well as new insights into the pK_a of **1**, was obtained. Understanding the way **1** and **2** differ from hydroxyl radicals, the archetype ROS, in the type of reaction that they undergo and in their site selection with unsaturated fatty acids and cholesterol was also obtained.

EXPERIMENTAL STUDIES

Bicarbonate Radical (1) Precursors. Research with oxime carbonates **3** showed that they release alkyl carbonate radicals $ROC(O)O^•$ on photolysis. These compounds are safe and have long shelf-lives and are thus promising precursors for the study of $HOC(O)O^•$ and $MeOC(O)O^•$ radicals. Compound PhCMeC═NOC(O)OH (**4**) would be expected to release radical **1** on irradiation together with the much less reactive[13−15] iminyl radical PhMeC═N• (Im) (Scheme 2).

Deprotection protocols with various derivatives of **3** [(Z = protecting group, route (a)] have not so far been successful, nor have experiments to generate radicals **5** that rearrange and/or eliminate to release **1** [route (b) in Scheme 2].[16] Before embarking on a project to further develop route (b), we decided to first forecast the structural integrity of **1** and to see how its reactivity would differ from that of **2** and from $HO^•$ radicals by examination of model $MeOC(O)O^•$ radicals and by DFT computations.

Scheme 2. Potential Lipid Soluble Precursors for Radical 1

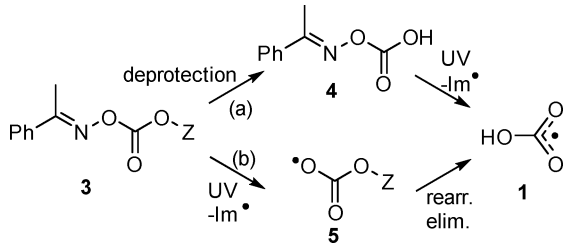

Methyl Carbonate Radical Additions to Aromatics and Decarboxylation Kinetics. The oxime carbonates **6a**,**b** were clear choices as precursors for the methyl carbonate (methoxycarbonyloxyl) radical **7**. They were prepared by a literature method[12a] from methyl chloroformate and the appropriate oxime. Solutions of each of **6a** and **6b** (0.1 mol) in *t*-butylbenzene containing 4-methoxyacetophenone (MAP, 1 equiv) as photosensitizer were purged with N_2 and UV irradiated in the resonant cavity of an EPR spectrometer. Neither $MeOC(O)O^•$ radicals nor $MeO^•$ radicals will be directly detectable by EPR in solution.[11a,17] The spectra actually disclosed the corresponding iminyl radical together with a second species having g = 2.0026, a(1H) = 34.5 G, a(1H) = 13.1 G, a(1H) = 9.3 G, a(1H) = 8.1 G, and a(1H) = 2.8 G. By analogy with literature data for other alkyl carbonate radicals,[11,12] we identify this as the *meta*-adduct radical **8** from addition of **7** to the solvent (Scheme 3).

Scheme 3. Generation and Reactions of Methyl Carbonate Radicals 7

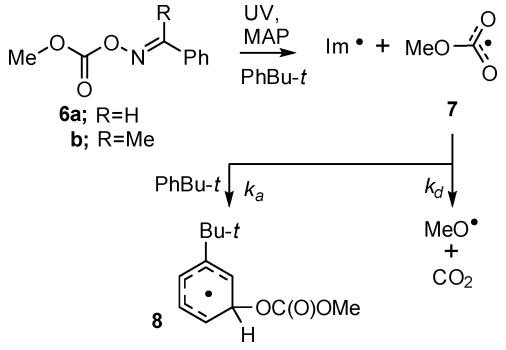

The concentration ratio [**8**]/[Im] was measured by simulation of spectra and is shown as a function of temperature in Figure 1.

With the **6b** precursor (open circles) the [**8**]/[Im] ratios were more scattered and less reliable because of the large difference in line width between **8** and Im in this case and the greater extent of overlap of their spectra. We therefore gave more weight to the data from **6a**. Equal numbers of Im and **7** radicals were formed in each initiation step, so the fact that the [**8**]/[Im] ratio was close to 1 at low temperatures (Figure 1, closed circles) indicated that the *meta*-addition of radical **7** to the solvent was very fast and complete. It follows, therefore,

DOI: 10.1021/jacs.5b10693
J. Am. Chem. Soc. 2015, 137, 16153−16162

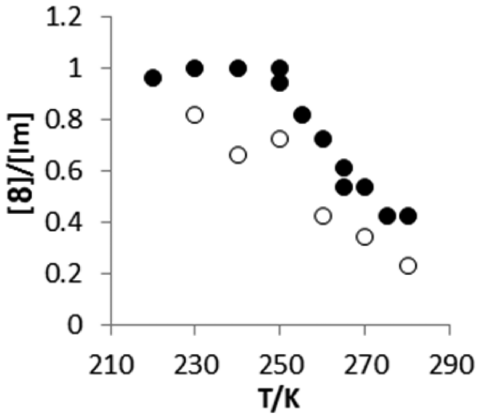

Figure 1. Data for decarboxylation of MeOC(O)O• radicals. Filled circles: data from oxime carbonate **6a**. Open circles: data from oxime carbonate **6b**.

that the amount of **8** equals the amount of **7** in solution. Above $T \sim 250$ K, the [**8**]/[Im] ratio decreased, and we attribute this to the onset of decarboxylative dissociation of **7** to MeO• and CO_2.

The rate constants of dissociation of **7** (k_d) were determined from measurements of the concentrations of **8** and Im in the falloff region. Making the steady-state approximation and assuming all termination steps were diffusion-controlled with rate constant $2k_t$, we obtained eq 1:[18]

$$k_d/2k_t = [\mathrm{MeO}] + [\mathrm{MeO}]^2/[\mathbf{7}] \quad (1)$$

Provided other reactions of **7** were insignificant, [**7**] = [**8**] and hence

$$k_d/2k_t = \{[\mathrm{Im}] - [\mathbf{8}]\} + \{[\mathrm{Im}] - [\mathbf{8}]\}^2/[\mathbf{8}] \quad (2)$$

Iminyl radicals terminate at the diffusion rate,[19] as do the other radicals in Scheme 4, and hence the use of Fischer's data for $2k_t$ [log A_t = 11.63 M^{-1} s^{-1}, E_t = 2.25 kcal mol^{-1}],[20] appropriately corrected for the difference in solvent viscosity,[21] was justified. Radical concentrations were determined from double integrations of the EPR spectra derived from precursor **6a** in the falloff region, and a satisfactory Arrhenius plot was

Scheme 4. Reaction of Methyl Carbonate Radical with Methyl Oleate

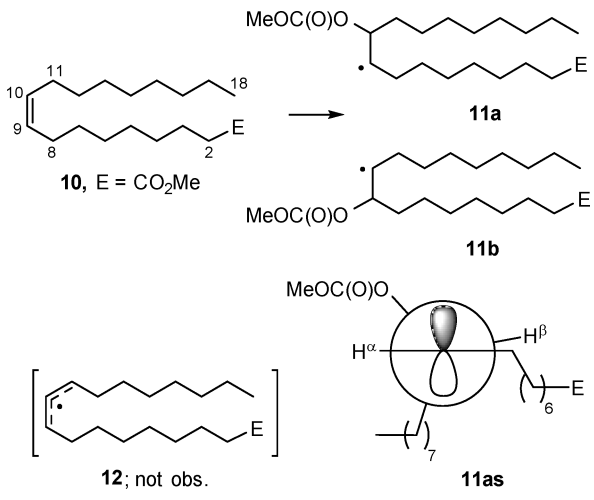

obtained (see Supporting Information) with parameters as follows:

$$\log(A_d/s^{-1}) = 13.9 \pm 1.8, \quad E_d = 14.6 \pm 2.2 \text{ kcal mol}^{-1}$$

$$k_d(300\text{ K}) = 1.8 \times 10^3\ s^{-1}$$

These results seem very reasonable because the measured activation barrier is close to experimental and to DFT computed barriers for dissociation of $PhCH_2OC(O)O^•$ radicals (12.9 ± 2.0 kcal mol^{-1}).[12a] It is evident, therefore, that **7** has sufficient structural integrity to take part in a range of chemical processes. Rate constants for H atom abstraction and addition reactions of alkyl carbonate radicals are on the order of[11b] 10^7 to 10^8 M^{-1} s^{-1}. Thus, radical **7** with a k_d of 1.8×10^3 will easily be persistent enough to engage in these processes at 300 K for substrate concentrations $>10^{-4}$ M.

There are interesting implications of these findings for the chemistry of bicarbonate radicals **1**. These will dissociate by β-scission to CO_2 and HO• radicals. The activation barriers and rates of radical β-scission reactions usually depend strongly on the thermodynamic stabilization of the released radical.[22] The HO• radical is *less thermodynamically stabilized* than MeO• or EtO• by 13.6 and 13.4 kcal mol^{-1}, respectively.[23] This gives a strong indication that the barrier to decarboxylative β-scission of the HOC(O)O• radical **1** will be considerably higher than that of **7** and the lifetime of **1** in nonpolar environments will be even greater. DFT computations[12] (see below) also predict a higher barrier. Once formed, therefore, bicarbonate radicals are expected to have ample lifetimes to attack lipid components and contribute, with other ROS, to their oxidative transformations. Our next step was to examine model reactions of radical **7** with organic substrates and lipid components to shed light on how bicarbonate radical oxidative processes could differ from those of HO• radicals and other ROS.

As shown above, addition of **7** to aromatics was rapid. We also found that **7** added very efficiently to furan, thiophene, and derivatives thereof (Table 1; see Supporting Information for sample spectra). The addition was selective for the 2- (or 5-) positions, and both 2- and 5-adduct radical isomers (**9**) were obtained in approximately equal amounts from 3-methylthiophene. In no case was an adduct radical from attack at a 3-position observed, although, because of the considerable noise levels, minor amounts would escape detection.

It is noteworthy that addition of **7** to the rings was preferred to abstraction of the benzyl-like H atoms of the CH_3 groups attached to both heterocycle types. Reaction with toluene was also examined. The spectra were too weak for definitive analysis but appeared to show a mixture of *ortho-*, *meta-*, and *para-*adduct radicals with again no sign of benzyl radicals from H-abstraction by the MOC(O)O• radicals. GC-MS analysis of the photolysate supported this conclusion (see Supporting Information).

Methyl Carbonate Radical Reactions with Lipid Components. Peroxidation, and the associated oxidative stress in organisms, is initiated when ROS damage lipid components of cells.[24] The mechanisms associated with this peroxidation have been intensively studied over many years.[25,26] The hydroxyl radical is the most reactive ROS, and it is well-established that this species initiates much peroxidation. It abstracts H atoms from allylic sites in monounsaturated lipid components such as oleic acid and cholesterol and from bis-allylic sites in di- and polyunsaturated fatty acids (PUFA). Subsequent chain propagation proceeds

DOI: 10.1021/jacs.5b10693
J. Am. Chem. Soc. 2015, 137, 16153−16162

Table 1. EPR Parameters of Adduct Radicals (9) of Methyl Carbonate Radicals and Heterocycles[a]

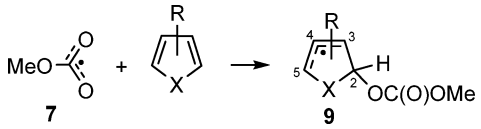

X, R	T/K	g-factor	a(H²)	a(H³)	a(H⁴)	a(H⁵)
O, H	240	2.0029	19.5	13.6	1.9	14.4
O, 2-Me	290	2.0022	18.4	13.9	1.6	12.7(3H)
O, 2-*t*-Bu	230	2.0030	19.7	13.9	1.7	
S, H	240	2.0046	18.6	11.9	2.3	13.7
S, 3-Me[b]	230	2.0040	17.4	12.5(3H)	2.5	13.7
S, 3-Me[b]	230	2.0040	18.1	11.2	2.4(3H)	14.0

[a]EPR hyperfine splitting (hfs) in gauss. [b]Isomeric radicals from addition at C-2 and C-5.

through addition of oxygen to the C-centered radicals, generating peroxyl radicals that then abstract H atoms, thus producing hydroperoxides. Our aim was to establish if bicarbonate radicals **1** would initiate in this same way, simply augmenting the regular peroxidation process, or if they could initiate alternative oxidative sequences ending in novel metabolites.

Our first evidence that radicals **7** behave differently came from a study of their reaction with hex-1-ene. When a solution of oxime carbonate **6b** and MAP in neat hex-1-ene was UV irradiated in the EPR cavity, the spectrum showed the PhMeC═N• radical (73%) and another radical (27%) with the following EPR parameters: g = 2.0027; a(1H) = 21.0 G, and a(4H) = 24.7 G at 290 K. We identify this as the adduct radical, $CH_3(CH_2)_3CH{\cdot}CH_2OC(O)OMe$. Surprisingly, none of the allylic radical from H-abstraction adjacent to the double bond could be detected. The predominant process was addition to the C═C double bond.

As a control experiment, we examined the reaction of **7** with the fully saturated fatty acid derivative methyl stearate [n-$C_{17}H_{35}C(O)OMe$]. The EPR spectrum taken during photolysis of a benzene solution (0.1 M in **6b** and 0.16 M in methyl stearate) at 292 K showed Im (87%) and a minor amount (13%) of a radical with g = 2.0028, a(1H) = 21.3 G, and a(4H) = 24.7 G. This is clearly a composite spectrum of the secondary radicals $-CH_2CH^{\bullet}CH_2-$ (s•) formed on H-abstraction from all 14 of the methylene groups in the chain that are flanked on both sides by CH_2 groups. This very weak spectrum contrasts with that reported for H atom abstraction from stearic acid by t-BuO• radicals (a model for ROS).[27] In that case, strong spectra of s• plus signals from the radicals α-to the COOH group (C_2, α-radicals) and adjacent to the CH_3 group (C_{17}, ω-1 radicals) were observed and indicated that t-BuO• radicals abstracted rapidly and unselectively from every site.

The EPR spectrum obtained from UV photolysis of a similar solution containing **6b**, methyl oleate (**10**), and MAP in PhH at 292 K is shown in Figure 2 (top).

In addition to Im radicals, a second radical with g = 2.0025, a(2H) = 26.1 G, a(1H) = 21.5 G, and a(1H) = 13.8 G was observed. This was readily identified as the adduct radical (**11a,b**) of MeOC(O)O• to the double bond of the methyl oleate (Scheme 4). A minor amount of secondary radicals s• (g = 2.0025, a(1H) = 21.5 G, and a(4H) = 24.5 G) was also observed. Spectra were obtained at several temperatures down to 220 K (with toluene as solvent for lower temperatures). Small amounts of peroxyl radicals (p; Figure 2, bottom) were detected with this solvent. The relative concentrations of the

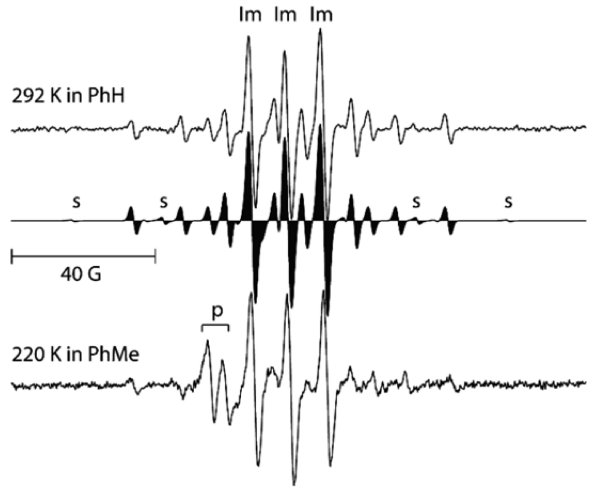

Figure 2. EPR spectra from **6b** and methyl oleate in solution. Top: experiment at 292 K in PhH. Center: Computer simulation (s indicates prominent peaks of secondary radicals; Im indicates PhMeC═N• radicals). Below: experiment at 220 K in PhMe (p indicates peroxyl radicals).

radicals determined at each temperature were as shown in Table 2. *None of allylic type radical* **12** from H-abstraction

Table 2. Relative Concentrations of Radicals Obtained on Photolysis of 6b and Methyl Oleate

T/K	solvent	Im (%)	**11a,b** (%)	s• (%)
292	PhH	60	36	4
273	PhH	51	49	<2
240	PhMe	54	46	<2
220	PhMe	63	37	<2

adjacent to the double bond (at C_8 or C_{11}) was detected.[28] The relatively large amounts of **11** showed that addition of radical **7** was rapid even at 220 K.

There was little change in the spectra up to 292 K, showing that the major pathway remained addition and that even dissociation of MeOC(O)O• did not compete. The small proportion of s• observed at 292 K demonstrated MeOC(O)-O• was less selective for addition at higher temperatures such that some H atom abstraction occurred.

The two radicals, **11a** and **11b**, formed on addition of MeOC(O)O• to either end of the double bond of **10** have extremely similar structures in the vicinity of their radical centers. Their EPR spectra will be indistinguishable, and the

DOI: 10.1021/jacs.5b10693
J. Am. Chem. Soc. 2015, 137, 16153−16162

experimental spectrum is probably a 50:50 mixture of the two.[29] The 13.8 G doublet hyperfine splitting (hfs) is from the single H^{β} of **11**, and its small magnitude (and the fact that this decreased to 12.5 G at 220 K) indicates this H^{β} lies close to the nodal plane of the p-orbital containing the unpaired electron. We can conclude that the preferred conformation is as shown in **11as**.[30] The majority of initiation in oleate peroxidation by other ROS types occurs by H atom abstraction adjacent to the double bond. For *t*-BuO$^{\bullet}$ radicals with oleate, for example, the allylic type species **12** (plus minor s$^{\bullet}$) were the only radicals detected by EPR spectroscopy.[31] There is, therefore, a striking contrast between the preferred addition reaction of MeOC(O)O$^{\bullet}$ radicals to C_9 and C_{10} of oleate and H-abstraction from C_8 and C_{11} preferred by other ROS.

The EPR spectrum obtained during a similar photolysis of **6b** and the doubly unsaturated methyl linoleate **13** in PhH at 293 K (Figure 3) contained Im (56%), adduct radical **14** [28%, *g* = 2.0025, *a*(2H) = 25.8 G, *a*(1H) = 21.7 G, and *a*(1H) = 14.4 G], and also pentadienic radical **15** (16%, *g* = 2.0025, *a*(2H) = 3.4 G, *a*(4H) = 8.0 G, *a*(2H) = 10.0 G, and *a*(1H) = 11.1 G]. Ester **13** (Scheme 5) contains four essentially equivalent sites for radical addition, and the resulting radicals would have indistinguishable EPR spectra, so the spectrum of **14** is probably a composite of all four. Allylic radicals are thermodynamically stabilized by about 10 kcal mol^{-1} more than secondary alkyl radicals, and pentadienic radicals are more stabilized by[23] about 15 kcal mol^{-1}. H atom abstraction from C_{11} in **13** will be, correspondingly, more facile. It is understandable, therefore, that the activation energy for bis-allylic H-abstraction by MeOC(O)O$^{\bullet}$ is sufficiently lowered for this to compete with addition.

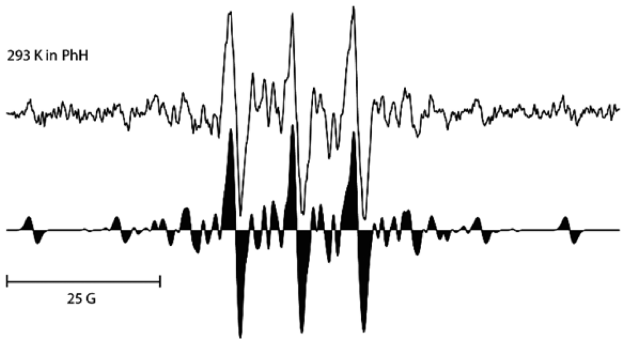

Figure 3. EPR spectra from **6b** and methyl linoleate **13**. Top: experiment at 293 K in PhH. Below: simulation including Im, adduct radical **14**, and pentadienic radical **15**.

Scheme 5. Reaction of Methyl Carbonate Radical with Methyl Linoleate (13) and Methyl γ-Linolenate (16)

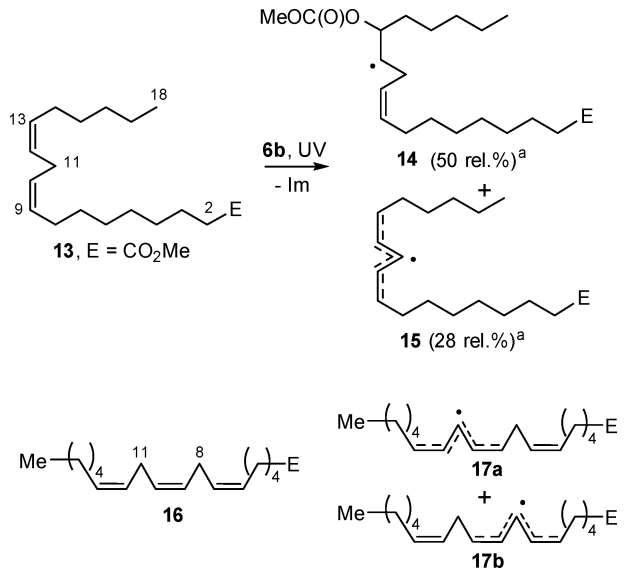

Again, there is a noteworthy contrast between MeOC(O)O$^{\bullet}$ and *t*-BuO$^{\bullet}$ (and other ROS) that exclusively abstracted H atoms from fatty ester **13**.[31]

The EPR spectra obtained from similar reactions of **6a** and **6b** with methyl γ-linolenate (**16**) contained mostly signals from the pentadienic radicals (**17a,b**) resulting from abstraction of H atoms at C_8 and C_{11} [50%: *g* = 2.0027, *a*(2H) = 3.4 G, *a*(4H) = 7.9 G, *a*(2H) = 10.0 G, and *a*(1H) = 11.3 G]. Only minor amounts of the adduct radicals were detected (see Supporting Information).

Cholesterol (**18**; Scheme 6) and its derivatives are also important oxidizable components of lipid structures.[26,32]

Scheme 6. Reaction of Methyl Carbonate Radical with Cholesterol

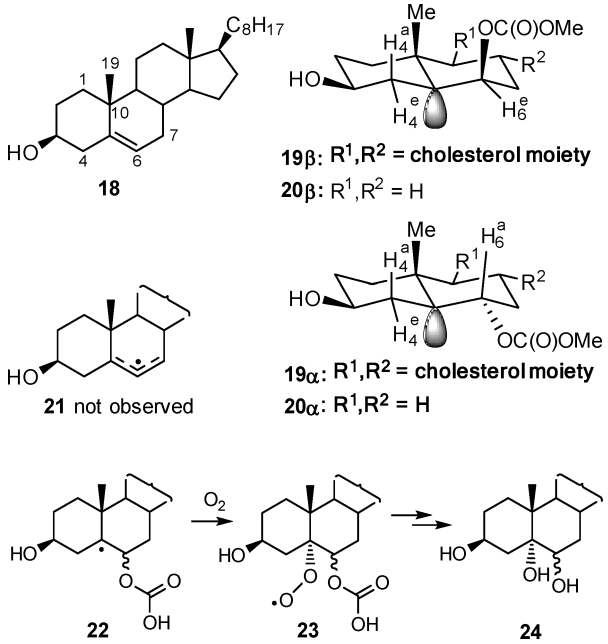

Peroxidation is initiated by transfer of an H atom from C_7, and the resulting allylic radicals **21** have been characterized by EPR spectroscopy.[33] H-transfer from C_4 has also been reported as well as peroxyl radical addition to the double bond at C_6, followed by epoxide formation via an S_Hi process.[34]

A solution of cholesterol (0.13 M) and **6b** (0.10 M) in PhH at 274 K on UV irradiation gave rise to the EPR spectrum of Figure 4.

Simulation showed this spectrum to be a composite of Im (58%) and two additional radicals both having *g*-factors of 2.0028 (characteristic of C-centered species) with the hfs in Table 3. None of the allylic radical **21** was detectable. To assist in identifying these species, the structures and hfs of model adduct radicals ***20α*** and ***20β*** were obtained from DFT computations at the UB3LYP/6-311+G(2d,p) level followed

DOI: 10.1021/jacs.5b10693
J. Am. Chem. Soc. 2015, 137, 16153−16162

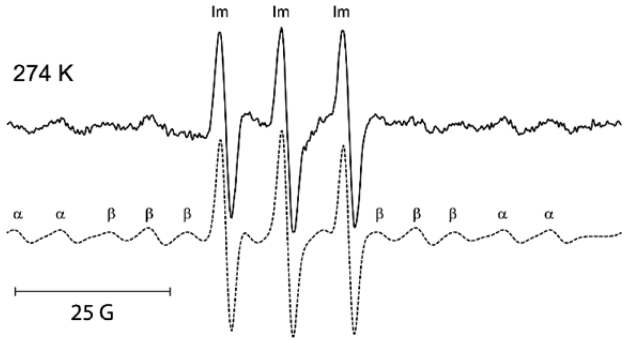

Figure 4. EPR spectra from **6b** and cholesterol in PhH at 274 K. Top: experimental spectrum during UV irradiation. Below: simulation including Im and adduct radicals **19*α*** and **19*β*** (prominent peaks marked α and β, respectively).

Table 3. EPR Parameters of Radicals from Addition of MeOC(O)O• to Cholesterol 18 (at C_6) and Model Species

radical	method	$a(H_4^e)$	$a(H_4^a)$	$a(H_6^{e\text{ or }a})$	$a(3H_{19})$
19*β* (29%)[a]	expt.	6.1	43.5	6.5	<1.4
20*β*	DFT[b]	5.3	42.1	6.2	1.4
19*α* (43%)[a]	expt.	7.5	42.8	36.9	<1.4
20*α*	DFT[b]	6.2	42.2	35.7	1.0

[a]Percent relative to Im concentration. [b]DFT isotropic Fermi contact hfs in gauss: geometry optimized at the UB3LYP/6-311+G(2d,p) level with single-point computation with the UB3LYP/aug-cc-pvtz method; note that all other computed hfs ≤1.0 G.

by single-point energies with UB3LYP/aug-cc-pvtz. Table 3 demonstrates the close correspondence between the computed hfs for models **20*β*,*α*** and the experimental parameters of the two spectral components. We conclude that these are adduct radical **19*β*** (29 rel. %) generated from approach by **7** from the β-face of the ring system and **19*α*** (43 rel. %) generated by approach from the α-face. These are bridgehead radicals, and, as expected, the hfs for the equatorial H^e atoms are comparatively small because they lie close to the nodal plane of the SOMO. The somewhat smaller amount of **19*β*** compared to **19*α*** is consistent with minor steric shielding of the β-face by the C_{19} Me group.

Radicals **1** and **7** are expected to exhibit very similar reactivities because they have very similar geometrical and electronic structures ($^2A'$ states). According to optimizations and natural population analyses at the CAM-B3LYP/6-31G(d,p) and CAM-B3LYP/6-311+G(2d,p) levels, respectively, the CO distances are the same within 1 pm, and atomic charges and spin densities of the terminal O atoms are identical within 0.01e. (See Figure S19 in the Supporting Information for a detailed comparison.) By analogy, therefore, bicarbonate radical **1** is expected to add to C_6 of cholesterol to produce the isomeric radicals **22** (Scheme 6). In a lipid structure, propagation of the peroxidation process will proceed by trapping oxygen and formation of peroxyl radicals **23**. Peroxyls are reductively converted to alcohols.[35] Furthermore, monoesters of carbonic acid, such as **23**, rapidly decarboxylate.[36] A major metabolite from peroxidation by bicarbonate radicals will, therefore, be the cholestane-3,5,6-triol isomer pair **24**. Further oxidation to 3β,5α-dihydroxy-cholestan-6-one and isomers may also take place.[37] Cholestane-3,5,6-triols, particularly cholestane-3β,5α,6β-triol, have been isolated from a number of natural products[38] and are biologically active in a variety of ways.[39] In contrast, peroxidation via the allylic radical **21** produces 7α- and 7β-hydroxycholesterol and 7-ketocholesterol as well as other metabolites.[26] Note, however, that some isomers of **24** can also be formed, in the absence of bicarbonate radicals, from peroxyl radical addition at C_6, subsequent 5,6-epoxide formation, and reductive epoxide ring opening.[26]

QM COMPUTATION OF BICARBONATE AND METHYL CARBONATE PROPERTIES

A QM computational study was undertaken in order to gain further insight into the structures, skeletal integrity, and acidity of the **1** ↔ **2** pair of radicals. From an initial validation study, it appeared that the CAM-B3LYP functional[40] could reproduce high-level ab initio benchmarks best (see Experimental Section below and Supporting Information for details); therefore, it was chosen to study decarboxylation and deprotonation reactions.

DFT Study of Alkyl Carbonate and Bicarbonate Decarboxylation. To obtain theoretical insight into how dissociation of ROC(O)O• radicals into CO_2 and RO• depends on the nature of R, we carried out computations with the species shown in Table 4. In accord with expectation for neutral

Table 4. Computed Reaction Enthalpies (ΔH_{298}), Free Energies (ΔG_{298}), and Activation Parameters ($\Delta H^{\ddagger}_{298}$, $\Delta G^{\ddagger}_{298}$) for CO_2 Loss from RO−CO_2• Radicals[a]

R	method[b]	medium	ΔH_{298}	ΔG_{298}	$\Delta H^{\ddagger}_{298}$	$\Delta G^{\ddagger}_{298}$
H	A	gas	5.6	−3.3	20.5	21.1
H	CBS-QB3	gas	3.4	−5.0	21.0	20.6
H	G4	gas	2.2	−6.2	19.9	19.6
H	A	*n*-hexane	5.3	−3.5	20.7	21.3
H	A	DCM	5.4	−3.5	20.8	21.5
H	A	H_2O	5.4	−3.5	20.9	21.5
Me	A	gas	−7.2	−17.4	13.6	13.0
Me	A	*n*-hexane	−7.4	−17.6	13.5	13.0
Me	A	DCM	−7.6	−17.8	12.8	12.3
Me	A	H_2O	−7.7	−17.8	12.6	12.2
Et	A	gas	−6.1	−15.9	12.8	11.9
Et	A	*n*-hexane	−6.8	−17.0	14.2	13.4
Et	A	DCM	−7.3	−17.6	13.9	13.0
Et	A	H_2O	−7.6	−17.8	12.7	11.8
Bn	A	gas	−7.3	−18.4	13.2	12.9
Bn	A	*n*-hexane	−7.9	−19.0	12.7	12.3
Bn	A	DCM	−8.3	−19.4	11.8	11.5
Bn	A	H_2O	−8.4	−19.4	11.5	11.2

[a]Values in kcal mol^{-1}. [b]"A" signifies the CAM-B3LYP/6-311+G(2d,p)//CAM-B3LYP/6-31G(d,p) method.

ROC(O)O• radicals, nonpolar (*n*-hexane), moderately polar (DCM), and even highly polar (water) solvents had minimal effects on the thermodynamic and kinetic energy parameters (Table 4). The dissociations for R = alkyl were computed to be exothermic, and their ΔG_{298} values were even more negative because of the increase in entropy accompanying β-scission. However, substantial energies of activation ($\Delta H^{\ddagger}$) and free energies of activation ($\Delta G^{\ddagger}$), were obtained for R = Me, Et, and Bn. This agrees with the significant radical lifetimes demonstrated by EPR spectroscopy. Confidence in the validity of the DFT computations was heightened by the good agreement of the computed $\Delta H^{\ddagger}$ values and experiment. Thus, for methyl carbonate radicals **7**, the DFT computed $\Delta H^{\ddagger}$ values of 13.6 and 13.5 kcal mol^{-1} for gas and *n*-hexane, respectively, were both within the error limits of our

DOI: 10.1021/jacs.5b10693
J. Am. Chem. Soc. 2015, 137, 16153−16162

experimental Arrhenius activation energy of 14.6 ± 2.2 kcal mol^{-1} in *t*-BuPh (see above). Similarly, for R = Bn, the DFT $\Delta H^{\ddagger}$ values of 13.2 and 12.7 kcal mol^{-1} in gas and *n*-hexane were also close to the experimental Arrhenius activation energy of 12.9 ± 2.0 kcal mol^{-1}.

This lends credence of the computed results for the bicarbonate radical itself. For this species (**1**), dissociation was found to be endothermic and only marginally exoergonic (by approximately −3.5 kcal mol^{-1}; Table 4). Furthermore, the computed $\Delta H^{\ddagger}$ and $\Delta G^{\ddagger}$ activation barriers (19.6−21.5 kcal mol^{-1}) were substantially greater (by 6.5 kcal mol^{-1} in the gas phase) than those for alkyl carbonate radicals. As mentioned above, the radical stabilization energy (RSE) of the released $HO^{\bullet}$ radical is less than that of $MeO^{\bullet}$ or $EtO^{\bullet}$ by 13.6 and 13.4 kcal mol^{-1}, respectively. It appears, therefore, that the *β*-scission barrier for bicarbonate exceeds that of methyl carbonate radicals by just under half of the difference in their RSEs, and this makes good sense.

Assuming $\log(A_d/s^{-1}) \approx 13$, typical of first-order dissociations, and an activation barrier of ca. 20 kcal mol^{-1} for $HOC(O)O^{\bullet}$ (**1**; Table 4) leads to an estimated k_d(300 K) ∼ 0.027 s^{-1} and a half-life of ∼25 s. This makes it abundantly clear that $HOC(O)O^{\bullet}$ radicals possess sufficient structural integrity to initiate multiple oxidative chains in a biological environment. Next, we turn to the expected acidity of this species in water.

Acidity of the Bicarbonate Radical. The acidities of oxoacids $XO_p(OH)_q$ increase as the number of oxygen ligands, p, increases. This reflects increasing resonance stabilization of the negative charge in the conjugate bases. Bell's rule for such acids [$pK_a = 8 - 5p$][41] applied to the bicarbonate radical suggests a pK_a of about −2 units. Recent experimental studies of the carbonate radical using optical pulse radiolysis,[6c] time-resolved resonance Raman spectroscopy,[6b] and EPR spectroscopy[6a] all indicate that the bicarbonate radical is highly acidic, with a pK_a less than zero. However, it has not been possible to experimentally determine the value.

Calculation of pK_a values is very computationally demanding because an error of only 1.4 kcal mol^{-1} in the free energy of deprotonation equates to an error of 1 pK_a unit at room temperature. Nevertheless, Armstrong et al.,[7] employing thermodynamic cycles and high level ab initio calculations, predicted a pK_a of −4.1 ± 1 units.

The main sources of error are the choice (and uncertainty) of the required free energy of hydration of the proton (usually taken from experiment) and the neglect of specific intermolecular interactions between the solvent and the conjugate acids and bases. To circumvent these problems, and in the spirit of Pulay and co-workers,[42] we predicted the pK_a of **1** based on linear correlation of computed deprotonation free energies ΔG_{A-HA} with experimental pK_as, using a set of 12 small carboxylic acids as reference. Gas- and aqueous-phase free energies of deprotonation (CAM-B3LYP and CPCM methods) as well as the correlations with experimental pK_as are collected in the Supporting Information. This procedure was designed to minimize any systematic errors in the individual predicted pK_a data.

Linear regression gave $pK_a = 0.151\Delta G_{A-HA} - 47.10$ (R^2 = 0.932) and $pK_a = 0.213\Delta G_{A-HA} + 0.428$ (R^2 = 0.919) for the gas- and aqueous-phase data, respectively (see Supporting Information). Extrapolation to the computed ΔG_{A-HA} for the bicarbonate radical afforded pK_a's of −0.39 and −0.69 from the gas and aqueous correlations, respectively. These estimates imply high acidity, although Bell's rule and previous computed values afforded even more negative values.

A possible shortcoming of such simple linear correlations is that they might become less reliable for very small and strong acids such as **1**, where specific interactions with the solvent would be most pronounced for the conjugate base with its very high charge density (**2** in our case). One way to account for this would be to refine the deprotonation energies by including specific microsolvating water molecules and check for convergence with increasing number of solvent molecules. The applicability of this approach to strong acids, however, is limited by their tendency to ionize spontaneously with just a few water molecules. HCl, for example, has been shown by experiment and DFT computations to dissociate upon addition of just four water molecules into a $Cl^-(H_2O)_3(H_3O^+)$ solvent-separated ion pair (SSIP) in the gas phase.[43] As expected, we observed the same type of spontaneous dissociation during attempted optimization of microhydrated clusters of **1** (see below), precluding quantitative assessment of the driving force for deprotonation upon hydration.

Several theoretical studies on microhydration of strong HX acids (X = F, Cl, Br, I),[44] perchloric,[45] formic,[46] nitric,[47] trifluoroacetic,[48] sulfuric,[49] and oxalic[50] acids, have established that, for strong mineral acids, indeed only a few microsolvating water molecules were needed to cause complete ionization. Furthermore, a trend toward a lower number of water molecules required for ionization (N_{aq}^{i}) as the acid increased in acidity was noted.[45] Theoretical estimation of N_{aq}^{i} is by no means easy because the number of possible conformations increases sharply as the number of water molecules increases. The potential energy surfaces for the interaction of HA with H_2O are rather shallow, leading to difficulties in establishing what are just local rather than global minima. Not surprisingly, as the foregoing literature demonstrates, some differences in N_{aq}^{i} have been reported for particular acids. A recent insightful article by Leopold surveys both theoretical and experimental approaches.[51] A plot of experimental pK_a values against N_{aq}^{i}, from published theoretical studies, is shown in Figure 5. The data was taken from high-level computations and, although alternative values can be found, high-quality N_{aq}^{i} do not differ from the chosen values by more than 1 unit. Thus, we feel the trend that emerges is real.

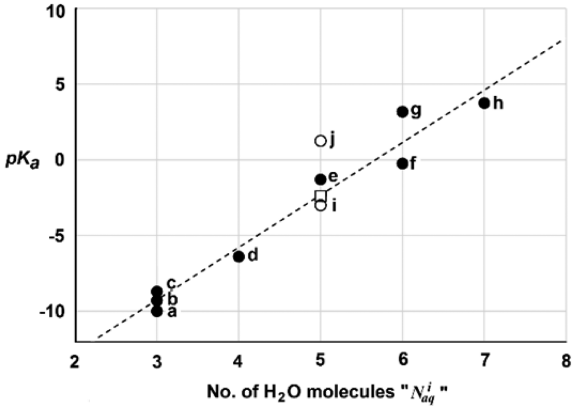

Figure 5. Plot of experimental pK_as of strong acids HX vs computed no. of microsolvating H_2O molecules required to induce their ionization. a, $HClO_4$; b, HI; c, HBr; d, HCl; e, HNO_3; f, CF_3CO_2H; g, HF; h, HCO_2H; i, H_2SO_4; j, oxalic acid (see text for literature references). Open square, $HOC(O)O^{\bullet}$ radical (**1**).

DOI: 10.1021/jacs.5b10693
J. Am. Chem. Soc. 2015, 137, 16153−16162

In Leopold's article,[51] spontaneous ionization of small acid−water clusters is qualitatively rationalized in terms of a thermodynamic cycle involving the energy for proton transfer from the neutral acid to H_2O and hydration energies of the various neutral and ionic species involved. Because hydration stabilizes the ionization products more strongly than the neutral precursors, it is entirely plausible (at least for strong acids) that the higher the proton-transfer energy, the more water molecules are needed to overcome this. One may thus expect $N_{aq}{}^{i}$ to correlate, at least qualitatively, with the gas-phase acidities (which vary appreciably for the acids studied; see Table S4 in the Supporting Information) and, hence, with pK_a.

The trend is remarkably linear, perhaps surprisingly so in view of the digital (integer) nature of $N_{aq}{}^{i}$. It is possible that nonlinearity will become apparent once data for a larger sample size becomes available. Straightforward linear regression of the data for the monoprotic acids yields the following relationship (eq 3) with $R^2 = 0.959$:

$$\mathrm{p}K_a = 3.46N_{aq}{}^{i} - 19.65 \quad (3)$$

Our objective, therefore, was to compute the number of microsolvating water molecules needed to bring about ionization of bicarbonate radical and hence obtain a further estimate of its pK_a.

Maity and co-workers[52] had reported structures for microsolvated carbonate radical anion clusters $[CO_3{}^{-\bullet}\cdot nH_2O]$, optimized to global minima at the B3LYP/6-311++G(d,p) level of theory, for n = 1−8. We chose Maity's $[CO_3{}^{-\bullet}\cdot 8H_2O]$ structure as our starting point, replaced the $CO_3{}^{-\bullet}$ with the bicarbonate radical, and optimized at CAM-B3LYP/6-31G-(d,p). Using the same input structure, we successively removed the outermost water molecules to obtain input structures for each smaller cluster. In this way, optimized cluster configurations were computed for the set of $[HOC(O)O^{\bullet}\cdot nH_2O]$ for n = 1−8 (see Supporting Information for examples).

In confirmation that bicarbonate radical is a strong acid, we observed that complete ionization was induced by only a few water molecules. The degree of ionization was assessed from the increasing O(acid)−H(acid) distance (d_{OH}) on increasing values of n. No significant increase in d_{OH} was observed for n = 1, 2, or 3. However, $HOC(O)O^{\bullet}$ underwent partial ionization with four water molecules, with d_{OH} increasing to 148% of its unsolvated length. Complete ionization occurred on addition of a fifth water molecule as d_{OH} increased to 336% of its original value. There was, then, no significant change in bond length for n > 5. Since the cluster with n = 4 (structure **b** in Figure S17 in the Supporting Information) appeared to be borderline, we conducted a more extensive search for its alternative minima. While a completely ionized SSIP was found to be very high in energy (isomer **c** in Figure S17), structure **b** rearranged during a Born−Oppenheimer molecular dynamics (BOMD) simulation to a configuration that turned out to be the most stable one upon optimization (structure **a** in Figure S17).[53] This structure, arguably the global minimum, had a "normal", barely elongated d_{OH}. We concluded that for $HOC(O)O^{\bullet}$ $N_{aq}{}^{i}$ = 5, and, from eq 3, this corresponds to a pK_a of approximately −2.4 (open square in Figure 5).[54] This result supports the conclusion that $HOC(O)O^{\bullet}$ has a pK_a value in the same range as H_2SO_4, but it is probably higher than that of HCl.

For further quantification of the pK_a value of **1**, free energy molecular dynamics simulations could be performed in a bulk aqueous environment, but these calculations would be rather expensive at the required level (CAM-B3LYP for an open-shell system). On the basis of our computations, we are confident, however, that the pK_a value of **1** will be around −2 to −1, helping to establish it as the strongest carboxylic acid.

CONCLUSIONS

We observed pleasing complementarity between spectroscopic investigations of the methyl carbonate radical **7**, as a model for the elusive bicarbonate radical **1**, and DFT computational studies of the latter. Radical **7** was shown to add very rapidly to aromatic and heterocyclic rings in preference to abstracting H atoms from benzylic-type sites. From radical concentration measurements, the activation energy for decarboxylative decomposition of **7** was found to be ∼14 kcal mol^{-1}. It follows that **7** has considerable structural integrity and a half-life of ∼0.4 ms at 300 K (in the absence of reactive substrates). The preference of **7** for addition over H-abstraction extended to monounsaturated lipid components including oleate and cholesterol. However, for lipid components containing "skipped" (i.e., 1,4-) diene moieties, abstraction of their bis-allylic H atoms took place alongside addition to their double bonds.

By analogy, the neutral bicarbonate radical **1** should actually decarboxylatively decompose more slowly and have a considerably longer half-life than **7**. DFT computations reinforced this conclusion. Activation enthalpies for β-scission of **1** were computed to be 20 ± 1.0 kcal mol^{-1} in gas and nonpolar media. It follows that, on generation in lipid microstructures, radical **1** will be a significant contributor to peroxidation. Furthermore, this peroxidation probably differs significantly from that by other ROS such as hydroxyl radicals. The latter initiate peroxidation by preferentially abstracting allylic and bis-allylic H atoms from mono- and polyunsaturated lipid components. However, because model radical **7** preferentially adds to double bonds, it is probable that **1** behaves likewise, particularly with monounsaturated lipid components. Important metabolites from peroxidation of cholesterol and oleate by **1** are, therefore, likely to be cholestane-3,5,6-triols and 9,10-dihydroxystearates, respectively. Both of these types of compounds are known to have a variety of biological activities.

Our DFT computational studies confirmed that **1** is a strong acid. pK_a's of −0.4 and −0.7 (gas- and aqueous-phase data, respectively) for **1** were obtained from linear correlations of computed deprotonation free energies (ΔG_{A-HA}) with the experimental pK_as of a set of strong acids. This may, however, underestimate the true acidity because of neglect of specific solvent interactions. These will be pronounced for the conjugate base **2** with its very high charge density. We discovered an intriguing linear relationship between the pK_as of strong acids and the integer numbers of water molecules required to induce ionization. DFT computations with the set of structures $[HOC(O)O^{\bullet}\cdot nH_2O]$ for n = 1−8 established that only five water molecules were needed to bring about complete ionization of the bicarbonate radical. Comparison of this finding with those for other strong acids gave a predicted pK_a of ca. −2.4 for **1**. It is interesting to note that this makes **1** *the strongest known* carboxylic acid: stronger than CF_3CO_2H (pK_a = −0.25) and stronger than the carboxyl radical ($^{\bullet}CO_2H$; pK_a = −0.2).[55] The high acidity of **1** can be attributed to the fact that in the conjugate base ($CO_3{}^{\bullet-}$) charge and electron density are distributed to three O-centers compared to only two O-centers in the conjugate bases ($RCO_2{}^{-}$) of most other carboxylic acids.

DOI: 10.1021/jacs.5b10693
J. Am. Chem. Soc. 2015, 137, 16153−16162

EXPERIMENTAL SECTION

Oximes and oxime carbonates were prepared and purified by the methods described previously.[12]

EPR spectra were obtained at 9.5 GHz employing a spectrometer fitted with a rectangular resonant cavity. Solutions of each oxime carbonate, MAP (1 equiv w/w), and substrate in PhH or *tert*-butylbenzene were prepared and sonicated if necessary. An aliquot (0.2 mL) was placed in a 4 mm o.d. quartz tube and deaerated by bubbling nitrogen for 15 min. Photolysis in the resonant cavity was by unfiltered light from a 500 W super pressure mercury arc lamp. EPR signals were digitally filtered and double integrated using the Bruker WinEPR software, and radical concentrations were calculated by reference to the double integral of the signal from a known concentration of the stable radical DPPH [1×10^{-3} M in PhMe], run under identical conditions. The majority of EPR spectra were recorded with 2.0 mW power, 0.8 G_{pp} modulation intensity, and gain of ca. 10^6.

All QM calculations were performed using the Gaussian 09 software package.[56] The high-quality quantum composite method, Gaussian-4,[57] was employed for exploratory computations (see Supporting Information). Geometries were fully optimized at the CAM-B3LYP/6-31G(d,p) level. Harmonic vibrational frequencies were computed to characterize the nature of the stationary points (transition states were further characterized through tracing the intrinsic reaction coordinate) and to evaluate thermodynamic corrections to enthalpies and free energies at standard pressure and temperature. Energies were refined at the CAM-B3LYP/6-311+G(2d,p) level for CAM-B3LYP/6-31G-(d,p) optimized geometries, denoted CAM-B3LYP/6-311+G(2d,p)//CAM-B3LYP/6-31G(d,p), in selected cases including the effects of a polarizable continuum to model bulk solvation (CPCM variant).[58] A BOMD simulation was performed for [DOC(O)O$^{\bullet}$·4D_2O] at the CAM-B3LYP/6-31G(d,p) level using the ChemShell program[59] as the MD driver. Starting from the minimum **b** (Figure S17), the system was propagated for 20 ps in the NVT ensemble (Nosé–Hoover chain set to 293 K, time step of 1 fs); selected structures along the trajectory were subjected to full CAM-B3LYP/6-31G(d,p) optimizations and energy calculations.

ASSOCIATED CONTENT

Supporting Information

The Supporting Information is available free of charge on the ACS Publications website at DOI: 10.1021/jacs.5b10693.

General experimental and synthesis section, sample EPR spectra, kinetic EPR data for methyl carbonate dissociation, validation of computational methods, DFT optimized structures and energies, and ^{1}H and ^{13}C NMR spectra of novel compounds (PDF)

AUTHOR INFORMATION

Corresponding Authors

*(M.B.) mb105@st-andrews.ac.uk
*(J.C.W.) jcw@st-andrews.ac.uk

Present Address

†(D.W.M.) Institute of Organic Chemistry and Biochemistry, Academy of Sciences of the Czech Republic, Flemingovo nam. 2, 166 10 Prague 6, Czech Republic.

Notes

The authors declare no competing financial interest.

ACKNOWLEDGMENTS

We thank EaStCHEM for funding and the EPSRC National Mass Spectrometry Service, Swansea. We are grateful to Luke Crawford and Dr. Herbert Früchtl for help with computing.

REFERENCES

(1) Waugh, A.; Grant, A. *Anatomy and Physiology in Health and Illness*, 11th ed.; Churchill Livingstone: Edinburgh, 2010.
(2) Medinas, D. B.; Cerchiaro, G.; Trindade, D. F.; Augusto, O. *IUBMB Life* **2007**, *59*, 255–262.
(3) (a) Lymar, S. V.; Hurst, J. K. *J. Am. Chem. Soc.* **1995**, *117*, 8867–8868. (b) Bonini, M. G.; Radi, R.; Ferrer-Sueta, G.; Ferreira, A. M. D. C.; Augusto, O. *J. Biol. Chem.* **1999**, *274*, 10802–10806.
(4) (a) Hodgson, E. K.; Fridovich, I. *Arch. Biochem. Biophys.* **1976**, *172*, 202–205. (b) Bonini, M. G.; Miyamoto, S.; Di Mascio, P.; Augusto, O. *J. Biol. Chem.* **2004**, *279*, 51836–51843.
(5) (a) Goss, S. P. A.; Singh, R. J.; Kalyanaraman, B. *J. Biol. Chem.* **1999**, *274*, 28233–28239. (b) Liochev, S. I.; Fridovich, I. *J. Biol. Chem.* **2002**, *277*, 34674–34678. (c) Ramirez, D. C.; Gomez-Mejiba, S. E.; Corbett, J. T.; Deterding, L. J.; Tomer, K. B.; Mason, R. P. *Biochem. J.* **2009**, *417*, 341–353. (d) Liochev, S. I.; Fridovich, I. *Free Radical Biol. Med.* **2010**, *48*, 1565–1569.
(6) (a) Chawla, O. P.; Fessenden, R. W. *J. Phys. Chem.* **1975**, *79*, 2693–2700. (b) Bisby, R. H.; Johnson, S. A.; Parker, A. W.; Tavender, S. M. *J. Chem. Soc., Faraday Trans.* **1998**, *94*, 2069–2072. (c) Czapski, G.; Lymar, S. V.; Schwarz, H. A. *J. Phys. Chem. A* **1999**, *103*, 3447–3450.
(7) Armstrong, D. A.; Waltz, W. L.; Rauk, A. *Can. J. Chem.* **2006**, *84*, 1614–1619.
(8) (a) Lapenna, D.; Ciofani, G.; Pierdomenico, S. D.; Giamberardino, M. A.; Cuccurullo, F. *FEBS Lett.* **2005**, *579*, 245–250. (b) Radi, R. *J. Biol. Chem.* **2013**, *288*, 26464–26472. (c) Lapenna, D.; Ciofani, G.; Cuccurullo, C.; Neri, M.; Giamberardino, M. A.; Cuccurullo, F. *Free Radical Res.* **2012**, *46*, 1387–1392.
(9) (a) Khairutdinov, R. F.; Coddington, J. W.; Hurst, J. K. *Biochemistry* **2000**, *39*, 14238–14249. (b) de Menezes, S. L.; Augusto, O. *J. Biol. Chem.* **2001**, *276*, 39879–39884.
(10) (a) Augusto, O.; Bonini, M. G.; Amanso, A. M.; Linares, E.; Santos, C. C. X.; De Menezes, S. L. *Free Radical Biol. Med.* **2002**, *32*, 841–859. (b) Berlett, B. S.; Chock, P. B.; Yim, M. B.; Stadtman, E. R. *Proc. Natl. Acad. Sci. U. S. A.* **1990**, *87*, 389–393.
(11) (a) Edge, D. J.; Kochi, J. K. *J. Am. Chem. Soc.* **1973**, *95*, 2635–2643. (b) Chateauneuf, J.; Lusztyk, J.; Maillard, B.; Ingold, K. U. *J. Am. Chem. Soc.* **1988**, *110*, 6727–6731.
(12) (a) McBurney, R. T.; Slawin, A. M. Z.; Smart, L. A.; Yu, Y.; Walton, J. C. *Chem. Commun.* **2011**, *47*, 7974–7976. (b) McBurney, R. T.; Harper, A. D.; Slawin, A. M. Z.; Walton, J. C. *Chem. Sci.* **2012**, *3*, 3436–3444. (c) McBurney, R. T.; Eisenschmidt, A.; Slawin, A. M. Z.; Walton, J. C. *Chem. Sci.* **2013**, *4*, 2028–2035.
(13) Fallis, A. G.; Brinza, I. M. *Tetrahedron* **1997**, *53*, 17543–17594.
(14) Bowman, W. R.; Cloonan, M. O.; Fletcher, A. J.; Stein, T. *Org. Biomol. Chem.* **2005**, *3*, 1460–1467.
(15) Walton, J. C. *Acc. Chem. Res.* **2014**, *47*, 1406–1416.
(16) DaBell, P. Report no. 1, *The Bicarbonate Radical in Biology and the Atmosphere*; University of St. Andrews, School of Chemistry: St. Andrews, 2014; pp 7–68.
(17) Symons, M. C. R. *J. Am. Chem. Soc.* **1969**, *91*, 5924.
(18) (a) Griller, D.; Ingold, K. U. *Acc. Chem. Res.* **1980**, *13*, 193–200. (b) Griller, D.; Ingold, K. U. *Acc. Chem. Res.* **1980**, *13*, 317–323.
(19) Portela-Cubillo, F.; Alonso-Ruiz, R.; Sampedro, D.; Walton, J. C. *J. Phys. Chem. A* **2009**, *113*, 10005–10012.
(20) (a) Schuh, H.-H.; Fischer, H. *Helv. Chim. Acta* **1978**, *61*, 2130–2164. (b) Schuh, H.-H.; Fischer, H. *Int. J. Chem. Kinet.* **1976**, *8*, 341–356.
(21) (a) Maillard, B.; Walton, J. C. *J. Chem. Soc., Perkin Trans. 2* **1985**, 443–450. (b) Bella, A. F.; Jackson, L. V.; Walton, J. C. *J. Chem. Soc., Perkin Trans. 2* **2002**, 1839–1843.
(22) Minozzi, M.; Nanni, D.; Walton, J. C. *J. Org. Chem.* **2004**, *69*, 2056–2069 and references cited therein..
(23) Hioe, J.; Zipse, H. Radical Stability – Thermochemical Aspects. In *Encyclopedia of Radicals in Chemistry, Biology and Materials*; Chatgilialoglu, C., Studer, A., Eds.; Wiley: Chichester, UK, 2012; Vol. *1*.
(24) Esterbauer, H. *Am. J. Clin. Nutr.* **1993**, *57*, 779S–786S.

DOI: 10.1021/jacs.5b10693
J. Am. Chem. Soc. 2015, 137, 16153–16162

(25) (a) Porter, N. A. *Acc. Chem. Res.* **1986**, *19*, 262−268. (b) Jahn, U.; Galano, J.-M.; Durand, T. *Angew. Chem., Int. Ed.* **2008**, *47*, 5894−5955. (c) Niki, E. *Free Radical Biol. Med.* **2009**, *47*, 469−484. (d) Gruber, F.; Mayer, H.; Lengauer, B.; Mlitz, V.; Sanders, J. M.; Kadl, A.; Bilban, M.; de Martin, R.; Wagner, O.; Kensler, T. W.; Yamamoto, M.; Leitinger, N.; Tschachler, E. *FASEB J.* **2010**, *24*, 39−48.
(26) Yin, H.; Xu, L.; Porter, N. A. *Chem. Rev.* **2011**, *111*, 5944−5972.
(27) Bascetta, E.; Gunstone, F. D.; Walton, J. C. *J. Chem. Soc., Perkin Trans. 2* **1984**, 401−406.
(28) Allyllic radical **12** probably saturates more readily and has narrower line widths than radicals **11** or $s^{\bullet}$; therefore, spectra were also scanned with low power and a small modulation intensity setting to make sure signals for **12** were not missed.
(29) Note also that each of **11a** and **11b** exists, of course, as a mixture of two enantiomers.
(30) For reviews of EPR determinations of radical conformations, see (a) Kochi, J. K. *Adv. Free Radical Chem.* **1975**, *5*, 189−317. (b) Walton, J. C. In *Encyclopedia of Radicals in Chemistry, Biology and Materials*; Chatgilialoglu, C., Studer, A., Eds.; Wiley: Chichester, UK, 2012; Vol. *1*, Chapter 7, pp 147−174.
(31) (a) Bascetta, E.; Gunstone, F. D.; Scrimgeour, C. M.; Walton, J. C. *J. Chem. Soc., Chem. Commun.* **1982**, 110−112. (b) Bascetta, E.; Gunstone, F. D.; Walton, J. C. *J. Chem. Soc., Perkin Trans. 2* **1983**, 603−613. (c) Kitaguchi, H.; Ohkubo, K.; Ogo, S.; Fukuzumi, S. *J. Am. Chem. Soc.* **2005**, *127*, 6605−6609.
(32) Smith, L. L. *Chem. Phys. Lipids* **1987**, *44*, 87−125.
(33) Sevilla, C.; Becker, D.; Sevilla, M. *J. Phys. Chem.* **1986**, *90*, 2963−2968.
(34) Smith, L. L. *Cholesterol Autoxidation*; Plenum Press: New York, 1981.
(35) (a) Brown, A. J.; Leong, S. L.; Dean, R. T.; Jessup, W. *J. Lipid Res.* **1997**, *38*, 1730−1735. (b) Ursini, F.; Maiorino, M.; Gregolin, C. *Biochim. Biophys. Acta, Gen. Subj.* **1985**, *839*, 62−70.
(36) (a) Pocker, Y.; Davison, B. L.; Deits, T. L. *J. Am. Chem. Soc.* **1978**, *100*, 3564−3567. (b) Reisenauer, H. P.; Wagner, J. P.; Schreiner, P. R. *Angew. Chem., Int. Ed.* **2014**, *53*, 11766−11771.
(37) (a) Watabe, T.; Sawahata, T. *J. Biol. Chem.* **1979**, *254*, 3854−3860. (b) Watabe, T.; Ozawa, N.; Ishii, H.; Chiba, K.; Hiratsuka, A. *Biochem. Biophys. Res. Commun.* **1986**, *140*, 632−637.
(38) (a) Datta, P. K.; Ray, A. K.; Barua, A. K.; Chowdhuri, S. K.; Patra, A. F. *J. Nat. Prod.* **1990**, *53*, 1347−1348. (b) D'Armas, H. T.; Mootoo, B. S.; Reynolds, W. F. *J. Nat. Prod.* **2000**, *63*, 1669−1671.
(39) (a) Liu, T.-F.; Lu, X.; Tang, H.; Zhang, M.-M.; Wang, P.; Sun, P.; Liu, Z.-Y.; Wang, Z.-L.; Li, L.; Rui, Y.-C.; Li, T.-J.; Zhang, W. *Steroids* **2013**, *78*, 108−114. (b) Tang, L.; Wang, Y.; Leng, T.; Sun, H.; Zhou, Y.; Zhu, W.; Qiu, P.; Zhang, J.; Lu, B.; Yan, M.; Chen, W.; Su, X.; Yin, W.; Huang, Y.; Hu, H.; Yan, G. *Steroids* **2015**, *98*, 166−172.
(40) Yanai, T.; Tew, D. P.; Handy, N. C. *Chem. Phys. Lett.* **2004**, *393*, 51−57.
(41) See, for example (a) Bell, R. P. *The Proton in Chemistry*, 2nd ed.; Cornell University Press: Ithaca, NY, 1973. (b) Miessler, G. L.; Tarr, D. A. *Inorganic Chemistry*, 2nd ed.; Prentice Hall: Upper Saddle River, NJ, 1999; p 164.
(42) Zhang, S.; Baker, J.; Pulay, P. *J. Phys. Chem. A* **2010**, *114*, 425−431 and 432−442..
(43) Gutberlet, A.; Schwaab, G.; Birer, O.; Masia, M.; Kaczmarek, A.; Forbert, H.; Havenith, M.; Marx, D. *Science* **2009**, *324*, 1545−1548.
(44) (a) Odde, S.; Mhin, B. J.; Lee, S.; Lee, H. M.; Kim, K. S. *J. Chem. Phys.* **2004**, *120*, 9524−9535. (b) Flynn, S. D.; Skvortsov, D.; Morrison, A. M.; Liang, T.; Choi, M. Y.; Douberly, G. E.; Vilesov, A. F. *J. Phys. Chem. Lett.* **2010**, *1*, 2233−2238.
(45) Weber, K. H.; Tao, F. M. *J. Phys. Chem. A* **2001**, *105*, 1208−1213.
(46) Maity, D. K. *J. Phys. Chem. A* **2013**, *117*, 8660−8670.
(47) Scott, J. R.; Wright, J. B. *J. Phys. Chem. A* **2004**, *108*, 10578−10585.
(48) Krishnakumar, P.; Maity, D. K. *J. Phys. Chem. A* **2014**, *118*, 5443−5453.
(49) Re, S.; Osamura, Y.; Morokuma, K. *J. Phys. Chem. A* **1999**, *103*, 3535−3547.
(50) Hermida-Ramon, J. M.; Cabaleiro-Lago, E. M.; Rodriguez-Otero. *Chem. Phys.* **2004**, *302*, 53−60.
(51) Leopold, K. R. *Annu. Rev. Phys. Chem.* **2011**, *62*, 327−349.
(52) Pathak, A. K.; Mukherjee, T.; Maity, D. K. *ChemPhysChem* **2008**, *9*, 2259−2264.
(53) Starting from conformer **b**, during the first 6 ps the MD simulation mainly sampled similar structures with slightly different orientations of the "dangling" OH bonds (with the shortest d_{OH} fluctuating between ca. 1.0 and 1.8 Å, mean value ca. 1.2 Å); at 6 ps, a rearrangement toward structure **a** occurred, after which the proton stayed firmly bound to the carbonate (mean $d_{OH} \approx 1.03$ Å).
(54) It should be noted that our calculations were done at a somewhat different level from the literature data summarized in Figure 5. At our level, however, we also find four water molecules required for the dissociation of HCl (as in refs 43 and 44), suggesting that the number of five water molecules required for **1** should be qualitatively reliable. This conclusion is reinforced by an exploratory computation for $HOC(O)O^{\bullet}\cdot 5H_2O$ at the ωB97X-D/6-31G** level (i.e., using the same functional as that in ref 48), where a somewhat different minimum is obtained than with CAM-B3LYP (see Supporting Information) but where ionization has occurred during optimization as well.
(55) Jeevarajan, A. S.; Carmichael, I.; Fessenden, R. W. *J. Phys. Chem.* **1990**, *94*, 1372−1376.
(56) Frisch, M. J.; Trucks, G. W.; Schlegel, H. B.; Scuseria, G. E.; Robb, M. A.; Cheeseman, J. R.; Scalmani, G.; Barone, V.; Mennucci, B.; Petersson, G. A.; Nakatsuji, H.; Caricato, M.; Li, X.; Hratchian, H. P.; Izmaylov, A. F.; Bloino, J.; Zheng, G.; Sonnenberg, J. L.; Hada, M.; Ehara, M.; Toyota, K.; Fukuda, R.; Hasegawa, J.; Ishida, M.; Nakajima, T.; Honda, Y.; Kitao, O.; Nakai, H.; Vreven, T.; Montgomery, J. A., Jr.; Peralta, J. E.; Ogliaro, F.; Bearpark, M.; Heyd, J. J.; Brothers, E.; Kudin, K. N.; Staroverov, V. N.; Kobayashi, R.; Normand, J.; Raghavachari, K.; Rendell, A.; Burant, J. C.; Iyengar, S. S.; Tomasi, J.; Cossi, M.; Rega, N.; Millam, J. M.; Klene, M.; Knox, J. E.; Cross, J. B.; Bakken, V.; Adamo, C.; Jaramillo, J.; Gomperts, R.; Stratmann, R. E.; Yazyev, O.; Austin, A. J.; Cammi, R.; Pomelli, C.; Ochterski, J. W.; Martin, R. L.; Morokuma, K.; Zakrzewski, V. G.; Voth, G. A.; Salvador, P.; Dannenberg, J. J.; Dapprich, S.; Daniels, A. D.; Farkas, O.; Foresman, J. B.; Ortiz, J. V.; Cioslowski, J.; Fox, D. J. *Gaussian 09*, revision D.01; Gaussian, Inc.: Wallingford, CT, 2009.
(57) Curtiss, L. A.; Redfern, P. C.; Raghavachari, K. *J. Chem. Phys.* **2007**, *126*, 084108.
(58) Barone, V.; Cossi, M. *J. Phys. Chem. A* **1998**, *102*, 1995−2001.
(59) (a) *ChemShell*, a Computational Chemistry Shell; Science and Technology Facilities Council: Cheshire, UK. www.chemshell.org. (b) Sherwood, P.; de Vries, A. H.; Guest, M. F.; Schreckenbach, G.; Catlow, C. R. A.; French, S. A.; Sokol, A. A.; Bromley, S. T.; Thiel, W.; Turner, A. J.; Billeter, S.; Terstegen, F.; Thiel, S.; Kendrick, J.; Rogers, S. C.; Casci, J.; Watson, M.; King, F.; Karlson, E.; Sjøvoll, M.; Fahmi, A.; Schäfer, A.; Lennartz, C. *J. Mol. Struct.: THEOCHEM* **2003**, *632*, 1−28.

DOI: 10.1021/jacs.5b10693
J. Am. Chem. Soc. 2015, 137, 16153−16162